Pflügers Archiv - European Journal of Physiology
https://doi.org/10.1007/s00424-020-02351-y

ORIGINAL ARTICLE

Effects of high-intensity interval training on adipose tissue lipolysis, inflammation, and metabolomics in aged rats

Lei Sun[1] · Fang-Hui Li[1] · Tao Li[2] · Zhu Min[1] · Luo-Dan Yang[2] · Hao-En Gao[1] · Da-Shuai Wu[1] · Tian Xie[1]

Received: 15 November 2019 / Revised: 8 January 2020 / Accepted: 20 January 2020

Abstract

High-intensity interval training (HIIT) is a time-efficient alternative to moderate-intensity continuous training (MICT) to improve metabolic health in older individuals. However, differences in adipose tissue metabolism between these two approaches are unclear. Here, we evaluated the effects of HIIT and MICT on metabolic phenotypes in aged rats. HIIT significantly decreased fat mass, increased percent lean mass, decreased fat-to-lean ratio, reduced serum high-sensitivity C-reactive protein, increased serum interleukin-10 levels, and decreased perirenal adipose tissue leptin compared with rats in the sedentary (SED) group. HIIT also increased pregnenolone, cortisol, and corticosterone in both adipose tissue and serum. Both exercise modalities enhanced hormone-sensitive lipase and adipose triglyceride lipase expression compared with the SED group and decreased palmitic acid, stearic acid, octadecadienoic acid, urea, 1-heptadecanol, and α-tocopherol. MICT was related to glycerolipid metabolism, whereas HIIT was related to steroid hormone biosynthesis. Overall, HIIT showed more favorable regulation of anti-inflammatory activity than MICT.

Keywords Aging · Inflammation · Adipose tissue · Metabolomics · High-intensity interval training · Moderate-intensity continuous training

Introduction

Aging is typically associated with increased adiposity and progressive redistribution of adipose tissue, characterized by a loss in subcutaneous adipose depot mass and a gain in abdominal white adipose tissue [29]. This adipose tissue has important endocrine roles involving secretion of different adipokines and inflammatory mediators, which regulate insulin sensitivity and low-grade inflammation [27]. These pathways can lead to the development of sarcopenia, cancer, and neurodegenerative, cardiovascular, and metabolic diseases [17, 27]. Thus, adipose tissue is a potent therapeutic target to combat the effects of aging and age-related diseases [27].

The beneficial effects of physical activity include improved energy balance, reduced adiposity, dysfunction of secreted adipokines, and subclinical inflammation [13]. Indeed, endurance training reduces inflammatory markers and the expression of senescence-associated secretory phenotype in white visceral adipose tissue, leading to improvement of locomotor activity in animal models with diet-induced fat cellular senescence [34]. However, no beneficial effects on the expression of lipolysis-related genes were observed in subcutaneous white adipocytes from middle-aged and elderly individuals who underwent combined endurance and strength training [25]. In obese postmenopausal women, high-intensity interval training (HIIT) is a time-efficient strategy to improve visceral adiposity and inflammatory markers when compared with combined strength and endurance training [26]. Paradoxically, mitochondrial DNA content and mitochondrial fat oxidation remain unchanged in the abdominal adipose tissue of healthy sedentary adults (aged 40 years) after HIIT for 6 weeks [21]. Notably, HIIT contributes to more favorable regulation of metabolism in the skeletal muscle [30] and liver [38] of elderly individuals, thereby improving clinical

This article is part of the special issue on *Exercise Physiology: future opportunities and challenges in Pflügers Archiv—European Journal of Physiology*

✉ Fang-Hui Li
12356@njnu.edu.cn

[1] School of Sport Sciences, Nanjing Normal University, No. 1 Wenyuan Road Qixia District, Nanjing 210046, People's Republic of China

[2] Laboratory of Laser Sports Medicine, South China Normal University, Guangzhou, China

Published online: 31 January 2020

outcomes in various aging-related metabolic disorders compared with moderate-intensity continuous training (MICT) [36]. However, there are currently no data linking the metabolic benefits of HIIT in aged adipose tissue, particularly compared with the MICT protocol, with the expansion of the sporting fields, therefore, which must seriously consider the need to establish animal models which may allow the design of more efficient and prevention-targeted preclinical studies on metabolomics.

Metabolomics is an expanding area in systems biology. Metabolites represent functional end products of gene expression which are closely related to global metabolic phenotypic changes [14]. Using gas chromatography/mass spectrometry (GC/MS), metabolomics analysis is a powerful and efficient technique for metabolic phenotypic investigation in exercise science [14], particularly when applied to adipose tissue, providing detailed information regarding the lipid composition [15]. Although few studies have focused on investigation of obesity-related markers, such as obesity-associated metabolites or adipocyte-derived peptides by GC/MS [15], no studies have systematically explored differences in metabolomic adaptations of aged adipose tissue to exercise training, particularly long-term HIIT versus MICT.

Accordingly, in this study, we evaluated the impact of long-term HIIT training on body composition, inflammatory mediators, adipokines, lipolysis genes, and metabolic phenotype in adipose tissue of aged rats and compared the results with those from a volume-matched MICT protocol.

Materials and methods

Animals

Eight-month-old female Sprague-Dawley rats ($n = 36$) were from Guangdong Medical Laboratory Animal Center (Foshan, Guangdong, China). The rats were housed at the Laboratory Animal Center, School of Sports Science and Physical Education, South China Normal University (SCNU), which was maintained under an artificial 12-h light-dark cycle (6:00 am to 6:00 pm) at constant room temperature (23 ± 1 °C). However, for our experiment, the rats were maintained on a reverse light cycle where the lights were off from 06:00 to 18:00 and on from 18:00 to 06:00. This was done to minimize animal stress and maximize data quality and translatability in order to avoid potential impact on adipocyte metabolism and hormone secretion from circadian rhythms disruption [3, 19]. The animals were housed in their respective groups in a collective cage and received water and standard laboratory chow ad libitum. All experiments were approved by the Ethics Committee on Animal Experimentation of the Guangdong Medical Laboratory Animal Center and followed the Guidelines for the Care and Use of Laboratory Animals. Experiments were approved by the Animal Experiment Ethical Inspection Form of Nanjing Normal University (IACUU-1903006).

Experimental design

All rats were raised until 18 months of age and then equally divided into sedentary (SED), MICT, and HIIT groups. The rats in SED group did not participate in any exercise treatment but were handled in a manner identical to that in the exercised groups. Overall, 12 rats were excluded from the study, including two rats from the SED group (owing to severe eye infections), four rats from the MICT group (three rats died from causes unrelated to exercise, two rats were excluded owing to severe claw infections), and six HIIT rats (two rats owing to nonadherence to the training protocol, and four rats because of severe claw and tail infections). The daily food consumption was described previously [22].

Training protocol

At the beginning, all rats were trained over the course of a 2-week acclimatization to run on an adapted motor-driven treadmill designed for rats (model FD000043; Flyde Apparatus, Guangzhou, China). During the first week of training, rats were individually placed into a treadmill lane at a 0° incline for a total of 10 min. At the start of the second week, rats ran at 10 m min^{-1}, progressing to 15 cm s^{-1} at a 0° incline for 30 min. Maximal oxygen uptake (VO_{2max}) was determined as reported previously [22].

MICT included 1 min of warm-up at a constant running speed of 10 m min^{-1}, which corresponded to 35–40% of VO_{2max}, followed by 45 min of constant running at 17 m min^{-1} (75–80% VO_{2max}) and cool down at a constant speed of 10 m min^{-1} for 1 min. HIIT included 4 min of low-speed running at 15 m min^{-1} (45–55% VO_{2max}), followed by 1 min of high-speed running at 25 m min^{-1} (90–95% VO_{2max}) at a 0% grade for 9 repetitions and cool-down at a constant speed of 10 m min^{-1} for 1 min. The total volume for the HIIT group was 3925 m $week^{-1}$, and the average intensity was about 75–80% VO_{2max}, matching that for the MICT group. To prevent avoidance and ensure exercise training, rats received a light electrical shock (6 mA) if they sat at the base of the treadmill. Within 2 weeks of training, the rates of exercise avoidance were minimal, and electrical shock was no longer needed. Exercise training sessions were held at the same time.

Body composition measurement and sample collection

To avoid the acute effects of the last bout of exercise training, dual-energy X-ray absorptiometry (DEXA; Unigamma X-ray

Plus, Cerro Maggiore, Milano, Italy) was carried out 48 h later. The rats were anesthetized with pentobarbital sodium 5% (50 mg kg^{-1} body weight [BW]) with heparin moistened syringes by intraperitoneal injection under dim infrared light within circadian time. Body fat and lean mass of animals at endpoint (26 months) were determined.

Following body composition assessment, the rats were anesthetized as previously described. Blood samples were collected from the abdominal aorta during the experiment. One milliliter of blood was collected in 1.5-mL RNase-free tubes mixed with 10 μL of the anticoagulant sodium heparin (5000 IU mL^{-1}) in order to obtain serum samples after centrifugation at 4000×*g* and 4 °C for 10 min for enzyme-linked immunosorbent assay (ELISA). After blood collection, perirenal adipose tissue (PAT) was rapidly excised by scalpel within 1 min postmortem and immediately weighed. One portion of each PAT was placed in clean centrifuge tubes, frozen in liquid nitrogen, and subsequently stored at − 80 °C until analysis of metabolic profiles via ELISA, reverse transcription polymerase chain reaction (RT-PCR), and western blotting were conducted. The remaining portion of each PAT was fixed in 10% buffered formalin for histological examination.

Inflammatory markers and adipokines from serum and adipose tissue

Serum (150 μL) and adipose tissue (100 mg) derived from PAT were homogenized at 4 °C for 15 min in tissue extraction buffer (60 μL) to determine the levels of interleukin (IL)-6 (#H007), IL-10 (#H009), adiponectin (ADP; #H179), leptin (#H174), and estradiol (#H102) using ELISA kits (Nanjing Jiancheng Bioengineering Institute, Jiangsu, China) according to the manufacturer's instructions. Additionally, serum hypersensitive C-reactive protein (hsCRP; #H126) and free fatty acids (FFAs; #A042-2) were also assessed using ELISA kits and an enzymatic colorimetric method (Nanjing Jiancheng Bioengineering Institute) according to the manufacturer's instructions. Serum and PAT pregnenolone (#ZC-54390), cortisol (#ZC-37081), and corticosterone (#ZC-37082) were evaluated using ELISA kits (Shanghai Zhuocai Bioengineering Institute, Shanghai, China), according to the manufacturer's instructions.

RNA extraction and RT-PCR

RNA was isolated from PAT using TRIzol reagent (cat. no. 9109; TaKaRa, Dalian, China), according to the manufacturer's instructions. Briefly, total RNA (1 μg) was reverse-transcribed using a cDNA synthesis kit (cat. no. RR047; TaKaRa) and quantified using a StepOnePlus REAL-TIME PCR system (Thermo Scientific; Rockford, IL, USA), according to the manufacturer's instructions. PCR was performed using a QuantiFast SYBR Green PCR Kit (cat. no. RR820A; TaKaRa) and a Mastercycler nexus X2 PCR (Eppendorf, Hamburg, Germany), according to the manufacturer's instructions. The relative abundances of peroxisome proliferator-activated receptor-γ (*PPAR-γ*), tumor necrosis factor-α (*TNF-α*), hormone sensitive lipase (*HSL*), and adipose triglyceride lipase (*ATGL*) mRNA were determined relative to the expression of the housekeeping gene glyceraldehyde phosphate dehydrogenase (*GAPDH*). The primer sequences are listed in Table 1.

Western blot analysis

Protein for each sample was separated using an electrophoresis apparatus (Bio-Rad, Hercules, CA, USA) with 4–20% sodium dodecyl sulfate-polyacrylamide and transferred to polyvinylidene difluoride membranes. The membranes were then blocked and incubated overnight at 4 °C with the following primary antibodies: anti-PPAR-γ (1:100; B-5; sc-271392; Santa Cruz Biotechnology, Dallas, TX, USA), anti-HSL (1:500; AF6403; Affinity Biosciences, Cincinnati, OH, USA), anti-ATGL (1:500; DF7756; Affinity Biosciences), anti-TNF-α (1:500; AF7014; Affinity Biosciences), and anti-P450scc (1:500; DF6569; Affinity Biosciences). After three washes, the membranes were incubated with horseradish peroxidase-conjugated secondary antibodies (1:10000 dilution; AF7021, Affinity Biosciences). Images of bound proteins were captured and analyzed using a Bio-Rad ChemiDoc XRS (Bio-Rad), and GAPDH was used as a loading control for the indicated proteins.

H&E staining

Adipose tissue from PAT was isolated and fixed for at least 24 h in 4–10% formaldehyde before embedding in paraffin.

Table 1 Primer sequences for quantitative real-time PCR

Gene name	Sequence 5′-3′ (forward)	Sequence 5′-3′ (reverse)
PPAR-γ	CGTGAAGCCCATCGAGGACATC	TCTGGAGCACCTTGGCGAACAG
TNF-α	GTGTCTGTGCCTCAGCCTCTTC	CCTCCTTGTTGGGACCGATC
HSL	CCTGCTGACCATCAACCGAC	CCTCGATCTCCGTGATATTCCAGA
ATGL	TGTGGCCTCATTCCTCCTAC	AGCCCTGTTTGCACATCTCT
GAPDH	TGCCGCCTGGAGAAACCTGC	TGAGAGCAATGCCAGCCCCA

Sections (5–7 mm; prepared using a Leica RM2135 microtome) were subjected to standard H&E staining and analyzed using CellD Olympus software (Olympus, Japan). At least 200 adipocytes per rat were analyzed for adipocyte surface area measurement. For adipocyte size quantification in PAT of rats in the HIIT, MICT, and SED groups, the investigator was blinded with regard to group allocation.

GC/MS sample preparation and analysis

PAT depots (10 mg) were added to 1000 μL extraction agent (acetonitrile/isopropanol/water). Next, 5 μL of 3 mg mL^{-1} myristic acid-d 27 solution was added, and samples were vortexed for 1 min, followed by ultrasonic extraction for 32 s and centrifugation at 4 °C for 5 min (15,000×*g*). Eight hundred microliters of the supernatant was then dried with liquid nitrogen, and a two-step derivation was performed as follows. First, the sample was added to 20 μL of 40 mg mL^{-1} methoxyamine hydrochloride/pyridine and incubated at 30 °C for 90 min. Next, 90 μL *N*-methyl-*N*-(trimethylsilyl) trifluoroacetamide containing 1% trimethylchlorosilane was added and incubated at 37 °C for 30 min, followed by centrifugation at 4 °C for 5 min at 13,000 rpm. Finally, 60 μL of the supernatant was subjected to analysis. All procedures were carried out on ice.

One-microliter aliquots of the derivatized solution were injected into an Agilent 7890A GC system (Agilent Technologies Inc.) with a splitless model. Separation was carried out on an Agilent DB5-MS fused silica capillary column (30 m × 250 μm × 0.25 μm), with high-purity helium as the carrier gas at a constant flow rate of 1 mL min^{-1}. The GC temperature programming was set to begin at 60 °C for 1 min and then increased to 300 °C (held for 10 min). Subsequently, the column effluent was introduced into the ion source of an Agilent 5975C mass selective detector. We set the mass selective quadrupole temperature at 150 °C and the ion source temperature at 230 °C. Electron impact ionization (− 70 eV) was used, with an acquisition rate of 20 spectra s^{-1} in the MS setting. MS detection was conducted with electron impact ionization mode in the full scan mode from *m*/*z* 50 to 500 [15].

Metabolomic data analysis and pathway analysis

For metabolomic data analysis, Agilent Chrom Station software (Agilent Technologies Inc.) was used to convert raw data into a NetCDF file format, and the file was then used for raw peak extraction, data baseline filtering, baseline calibration, peak alignment, deconvolution analysis, peak identification, and peak area integration. The retention time index (RI) method was used for peak identification, and the RI tolerance was set to 5000. In order to dislodge the noise data and conduct a better analysis of downstream data, all raw data were filtered by retaining the treatments with a null value of less than or equal to 50%. Raw data were filtered by retaining the treatments with a matching degree of greater than or equal to 80%, yielding reliable results.

Multivariate analysis, including principal component analysis (PCA) and orthogonal correction partial least squares discriminant analysis (OPLS-DA), was conducted using MetaboAnalyst 4.0. Unsupervised pattern recognition method PCA was applied to the unit variance-scaled spectral data. Then, to maximize class discrimination, the data were further analyzed using the supervised pattern recognition OPLS-DA method [14]. This was carried out in order to reduce the effects of irrelevant metabolite variability and to identify adipose tissue metabolites contributing to differences in the MICT and HIIT groups. OPLS-DA produced three key parameters: R2X (the cumulative model variation in Y), R2Y (the cumulative model variation in Y), and Q2 (the cumulative predicted variation). The parameters for quantifying this OPLS-DA model (R2X, R2Y, and Q2Y) were all positive. The OPLS-DA model was considered robust and to have predictive reliability as these parameters approached 1.0. The variables farthest from the origin in the S-plot represented metabolites that differed significantly between the two treatments. Moreover, greater deviation of the variables from the origin indicated higher variable importance in the projection (VIP) values. When the VIP value was greater than 1.0, the variable was considered a contributor for the classification. Significantly changed metabolites in both MICT and HIIT groups compared with the SED group were identified based on VIP values from OPLS-DA analysis and statistical analysis ($VIP > 1$, $P < 0.05$).

Significantly altered metabolites in the two groups were imported into MetaboAnalyst 4.0 to conduct pathway analysis. Pathway analysis and visualization for significantly changed metabolites based on the Kyoto Encyclopedia of Genes and Genomes (KEGG; http://www.genome.jp/kegg/) database were used to identify the most significantly altered metabolic pathways [14].

Statistical analysis

Experimental data were expressed as means ± standard deviations (SDs), and statistical analyses were performed with GraphPad Prism 7.0 (GraphPad Software Inc.). Training intervention differences among SED, MICT, and HIIT groups were assessed via one-way analysis of variance (ANOVA) followed by Tukey's post-hoc test. Student's *t* tests were carried out for comparisons of the MICT and HIIT groups with the SED group. Pearson's correlation tests were used to assess correlations between variables and were performed in R software. For all tests, *P* values of less than 0.05 were considered significant.

Results

Body composition and morphological measurement of adipocyte size

Body weight and body composition as determined using DEXA after 8 months of exercise training are shown in Fig. 1 and Table 2. Fat mass ($P = 0.028$; Fig. 1b), fat mass-to-BW ratio ($P = 0.039$; Fig. 1c), and fat-to-lean mass ratio ($P = 0.024$; Fig. 1d) were lower in the HIIT group than in the SED group. There were significant decreases in the sizes of adipocytes and expansion capacity from PAT in both the HIIT ($P = 0.001$; Fig. 1f) and MICT ($P = 0.020$; Fig. 1f) groups compared with those in the SED group. These findings suggested that 8 months of HIIT suppressed the aged-induced increases in fat mass, in contrast to the results in the MICT group. And HIIT reduction in fat cell size in particular was also greater than that observed in the MICT.

Inflammatory cytokines and adipocytokines

Levels of inflammatory markers, steroid hormones, adipocytokines, estradiol, and circulating FFAs in the PAT and serum are shown in Fig. 2. HIIT significantly increased pregnenolone (Fig. 2f, n), cortisol (Fig. 2g, o), and corticosterone (Fig. 2h, p) in both the PAT and serum compared with those in the SED and MICT groups, and MICT significantly increased pregnenolone ($P = 0.013$; Fig. 2n) and corticosterone ($P = 0.035$; Fig. 2p) compared with those in the SED group only in the serum. Lower PAT leptin levels were observed in the HIIT group compared with those in the SED group ($P = 0.042$; Fig. 2d), and higher PAT estradiol levels were observed in the MICT ($P = 0.004$; Fig. 2e) and HIIT ($P = 0.001$; Fig. 2e) groups compared with those in the SED group. These data suggest that HIIT is more effective for improving steroid hormone biosynthesis than MICT in aged rats. However, HIIT did not augment PAT estradiol biosynthesis compared to those in the MICT group.

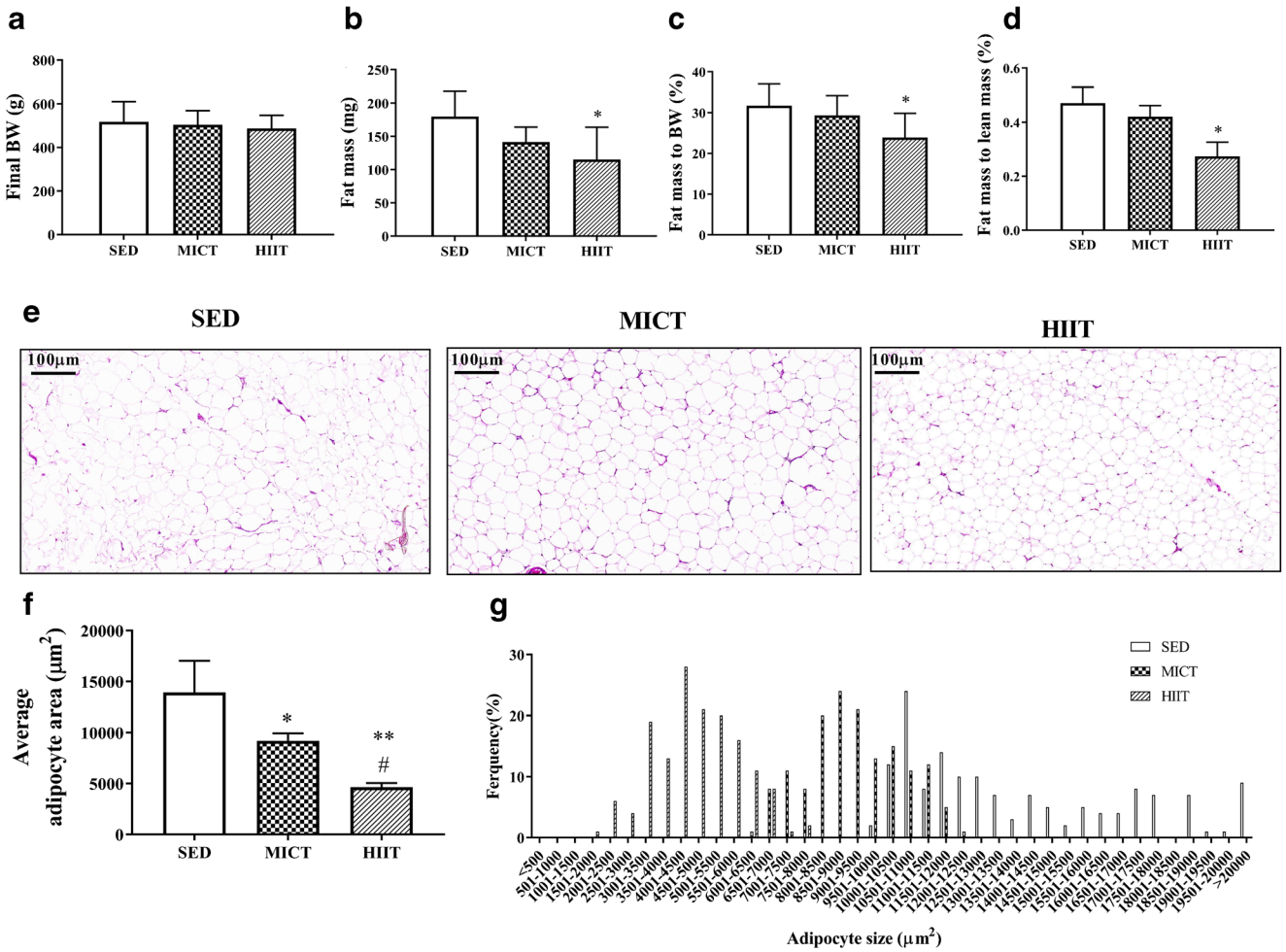

Fig. 1 Effects of the MICT and HIIT protocols on body composition and average adipocyte area. Changes in final BW (**a**), fat mass (**b**), fat mass-to-BW ratio (**c**), fat mass-to-lean mass (**d**), H&E stain (**e**), average adipocyte area (**f**), and adipocytes area frequency (**g**). SED sedentary control group, MICT moderate-intensity continuous training group, HIIT high-intensity interval training group, BW body weight, H&E stain hematoxylin and eosin stain. The data were analyzed by one-way ANOVA followed by Tukey's post-hoc test. Data are presented as means ± SDs. $^{*}P < 0.05$ versus SED; $^{**}P < 0.01$ versus SED; $^{\#}P < 0.05$ versus MICT; $^{\#\#}P < 0.01$ versus MICT

Table 2 Effect of the MICT and HIIT protocols on relative tissue weight

	SED ($n = 10$)	MICT ($n = 8$)	HIIT ($n = 6$)
Relative uterus **weights (mg g^{-1})**	0.037 ± 0.02	0.04 ± 0.02	0.04 ± 0.01
Relative liver **weights (mg g^{-1})**	2.50 ± 0.34	2.21 ± 0.22	2.57 ± 0.20
Relative ovary **weights (mg g^{-1})**	0.01 ± 0.003	0.025 ± 0.005**	0.018 ± 0.01
Relative heart **weights (mg g^{-1})**	0.26 ± 0.05	0.27 ± 0.02	0.26 ± 0.01
Relative perirenal adipose **weights (mg g^{-1})**	6.09 ± 2.72	7.61 ± 1.85	7.29 ± 1.42

Values are reported as the means ± SD. Relative tissue weight = tissue weight (mg)·final BW (g)$^{-1}$ × 100. Groups: SED, sedentary; MICT, moderate-intensity continuous training; and HIIT, high-intensity interval training. SED, MICT, and HIIT groups were assessed via one-way ANOVA followed by Tukey's post-hoc test

**$P < 0.01$ with respect to SED group

In serum, lower levels of the pro-inflammatory marker hsCRP were observed in the HIIT group compared with those in the SED ($P = 0.019$; Fig. 2i) and MICT ($P = 0.013$; Fig. 2i) groups. However, IL-10 levels were higher in the HIIT group than in the SED group ($P = 0.007$; Fig. 2k) and MICT group ($P = 0.036$; Fig. 2k), whereas lower estradiol levels were observed in the HIIT ($P < 0.0001$; Fig. 2l) and MICT ($P < 0.0001$; Fig. 2l) groups compared with those in the SED group. Additionally, HIIT rats showed higher serum FFA levels than SED ($P = 0.0001$; Fig. 2m) and MICT ($P = 0.001$; Fig. 2m) rats. Therefore, consistent with the results of anti-inflammatory factor IL-10 and steroid hormone, HIIT significantly attenuated this aged-induced pro-inflammatory response.

Differences in nontargeted metabolomic profiles between MICT and HIIT

After strict quality control and identification, 60 metabolites were obtained across all samples. In further analysis, samples from the MICT and HIIT groups could be clearly distinguished from samples from the SED group according to both PCA and OPLS-DA analysis (Fig. 3). As shown in Fig. 3 a and d, PCA revealed that PCA axes 1 and 2 accounted for 47.4% and 34.5% of the total variation, respectively, whereas in Fig. 3d, PCA axes 1 and 2 accounted for 47.1% and 25.3% of the total variation, respectively. Greater agglomeration of samples within the same group indicated smaller differences in metabolism for samples within the same group, whereas greater separation of samples from different groups indicated higher sample reproducibility and greater differences in metabolism between the two groups. To maximize the discrimination, OPLS-DA analysis was carried out. As demonstrated by OPLS-DA score plots, samples from MICT and HIIT groups compared with the SED group were separated into distinct clusters, indicating that the observed alterations in metabolic profiles were related to the types of exercise (Fig. 3b, e). OPLS-DA loading plots revealed that this model was efficient and showed clear separation between the MICT and SED groups (R2X = 0.28, R2Y = 0.84, and Q2 = 0.76; Fig. 3b). OPLS-DA loading plots indicated that this model was also efficient and showed clear separation between HIIT and SED groups (R2X = 0.20, R2Y = 0.79, and Q2 = 0.58; Fig. 3e). As shown in Fig. 3, PCA and OPLS-DA of PAT samples showed that rats in the SED group were clustered far away from rats in the HIIT or MICT group, indicating that there were notable metabolic changes induced by both exercise modalities.

Nine and six metabolites were finally selected as significantly altered metabolites from both MICT and HIIT groups, respectively, compared with the SED group (Fig. 3c, f). Among these metabolites, palmitic acid, stearic acid, and octadecadienoic acid decreased, whereas lumichrome and α-tocopherol increased in both the MICT and HIIT groups, demonstrating similar metabolic changes between the two training groups. Notably, palmitoleic acid, urea, and 1-heptadecanol decreased, whereas glycerol increased in the MICT group (Table 3). Additionally, cholesterol increased in the HIIT group (Table 4) compared with that in the SED group, clearly suggesting that both exercise modalities induced specific metabolic changes.

As shown in Fig. 4a, both palmitic acid and palmitoleic acid were positively correlated with stearic acid and octadecadienoic acid and negatively correlated α-tocopherol. Moreover, palmitic acid was positively correlated with palmitoleic acid in the MICT group. As shown in Fig. 4d, palmitic acid, stearic acid, and octadecadienoic acid were negatively correlated α-tocopherol, and cholesterol was positively correlated with α-tocopherol in the HIIT group.

To visualize data in the biological context of metabolic pathways, pathway analysis related to different metabolites was conducted using MetaboAnalyst 4.0 software and KEGG (Fig. 4b, e). MICT pathway analysis showed that these metabolites were mainly involved in glycerolipid metabolism ($P = 0.025$, impact = 0.281). In contrast, HIIT pathway analysis showed that these metabolites were mainly involved in steroid hormone biosynthesis ($P = 0.006$, impact = 0.017), primary bile acid biosynthesis ($P = 0.006$, impact = 0.037), glycerolipid metabolism ($P = 0.087$, impact = 0.281), and steroid biosynthesis ($P = 0.006$, impact = 0.054).

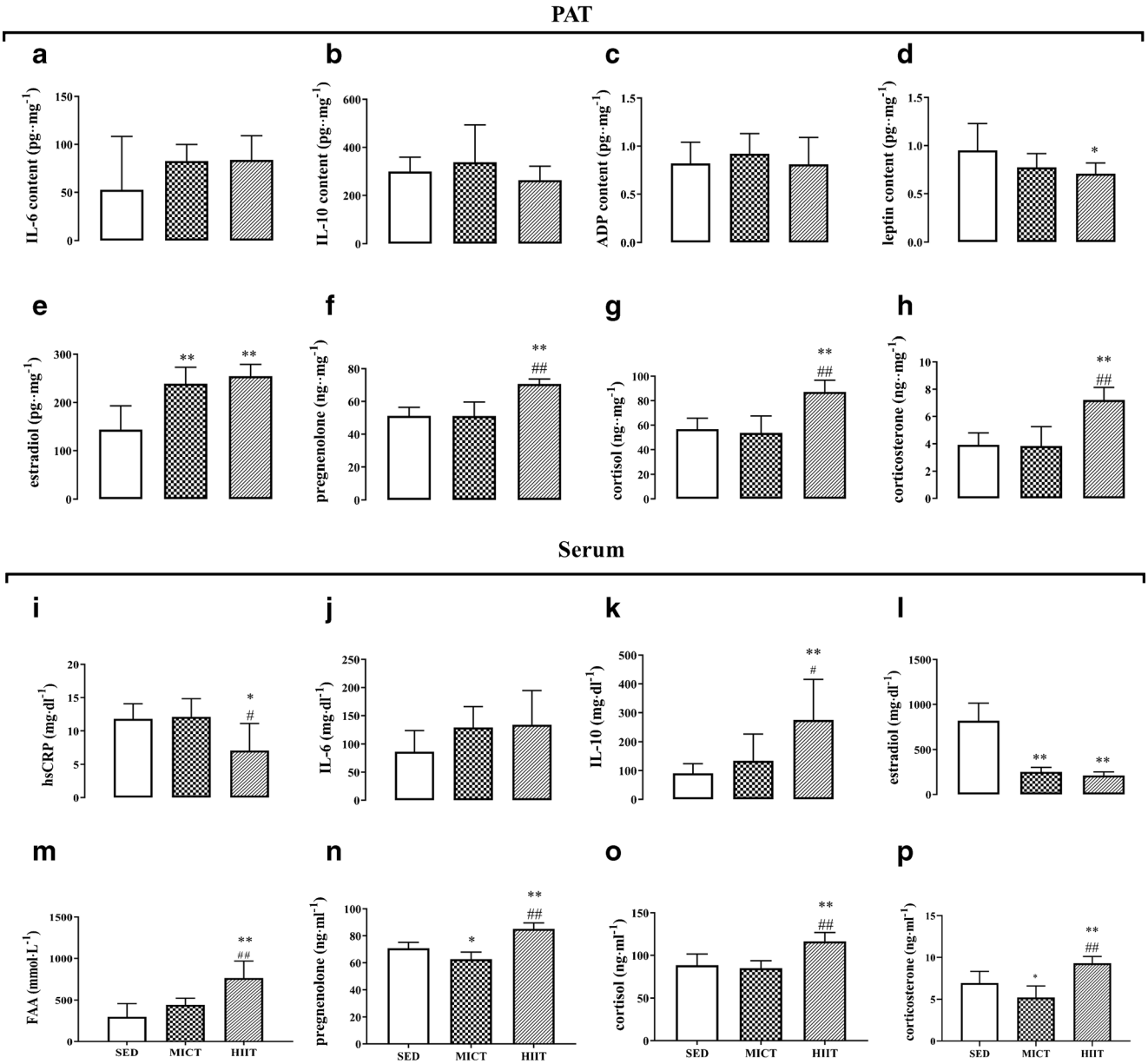

Fig. 2 Effects of the MICT and HIIT protocols on inflammatory markers and adipocytokines. IL-6 (**a**), IL-10 (**b**), ADP (**c**), leptin (**d**), estradiol (**e**), pregnenolone (**f**), cortisol (**g**), and corticosterone (**h**) in PAT; hsCRP (**i**), IL-6 (**j**), IL-10 (**k**), estradiol (**l**), FFA (**m**), pregnenolone (**n**), cortisol (**o**), and corticosterone (**p**) in serum. SED sedentary control group, MICT moderate-intensity continuous training group, HIIT high-intensity interval training group, PAT perirenal adipose tissue, IL-6 interleukin 6, IL-10 interleukin 10, ADP adiponectin, hsCRP hypersensitive C-reactive protein. The data were analyzed by one-way ANOVA followed by Tukey's post-hoc test. Data are presented as means ± SDs. $^{*}P < 0.05$ versus SED; $^{**}P < 0.01$ versus SED; $^{\#}P < 0.05$ versus MICT; $^{\#\#}P < 0.01$ versus MICT

Protein and mRNA levels of HSL, ATGL, TNF-α, and PPAR-γ

The expression levels of HSL, ATGL, TNF-α, and PPAR-γ mRNA and protein in fat tissues are shown in Fig. 4c and f. As shown in Fig. 4c, the HIIT and MICT groups show significantly higher levels of *HSL* and *ATGL* mRNA and significantly lower levels of *TNF-α* mRNA compared with the SED group; additionally, *HSL* mRNA levels were significantly higher ($P < 0.0001$) in the HIIT group than in the MICT group. Moreover, *PPAR-γ* mRNA levels were significantly higher ($P < 0.0001$) in the HIIT group than in the MICT and SED groups.

As shown in Fig. 4f, western blot analysis further confirmed this effect on the protein expression of HSL, ATGL, PPAR-γ, and TNF-α, suggesting that HIIT may be more effective for improving the expression of lipolytic enzymes in PAT than MICT in aged rats. Additionally, the protein levels of p450scc ($P = 0.011$) were higher in the HIIT group than in the MICT group, consistent with the results of downstream

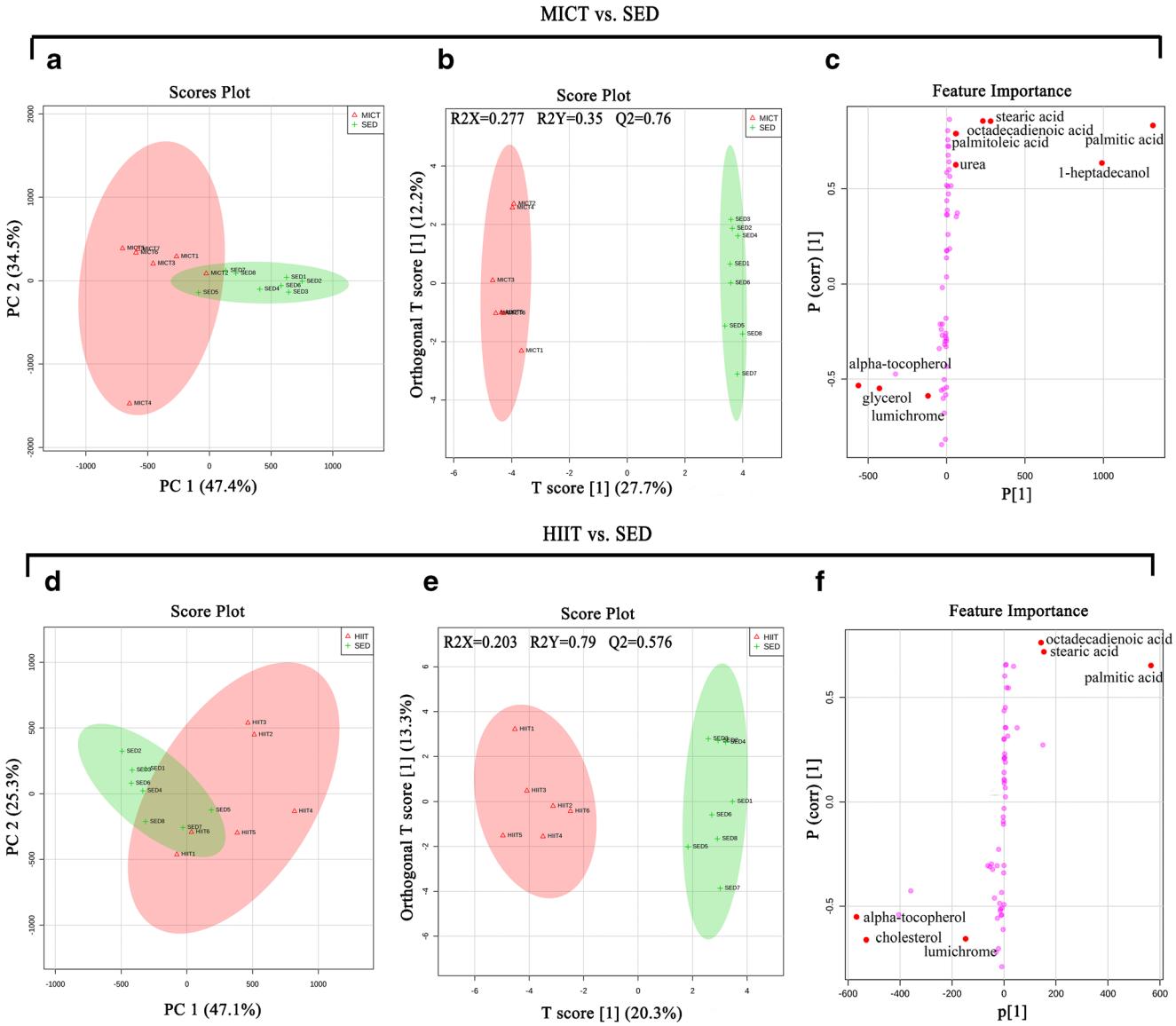

Fig. 3 Multivariate statistical analysis. PCA of PAT metabolites from MICT versus SED (**a**), OPLS-DA of PAT metabolites from MICT versus SED (**b**), S-PLOT analysis of 10 metabolites from MICT versus SED (**c**), PCA of PAT metabolites from HIIT versus SED (**d**), OPLS-DA of PAT metabolites from MICT versus SED (**e**), and S-PLOT analysis of nine metabolites from HIIT versus SED (**f**). SED sedentary control group, MICT moderate-intensity continuous training group, HIIT high-intensity interval training group, PAT perirenal adipose tissue

pregnenolone (Fig. 2f, n), cortisol (Fig. 2g, o), and corticosterone (Fig. 2h, p). Similar results were found for mRNA levels in the MICT and HIIT groups, and exercise significantly improved steroid hormone biosynthesis pathways in aging adipose tissue.

Discussion

In this study, we identified several similar metabolites involved in glycerolipid metabolism and antioxidants in the MICT and HIIT groups and showed that steroid hormone biosynthesis pathways were upregulated by HIIT. Additionally, HIIT improved body composition in aged rats, potentially through upregulation of the PPAR-γ-dependent functional regulatory node of the lipolytic axis in aged adipocytes. Moreover, we confirmed HIIT may contribute to positive regulation of anti-inflammatory activity via induction of steroid hormone biosynthesis pathways.

Using GC/MS analysis, we determined the metabolic profiles of adipose tissues in order to elucidate the metabolite-specific changes in response to HIIT and MICT. Our results showed that palmitic acid, octadecadienoic acid, stearic acid, lumichrome, and alpha-tocopherol exhibited similar changes induced by both exercise modalities. In contrast, urea, 1-heptadecanol, palmitoleic acid, and glycerol were specifically

Table 3 Changes in metabolites in adipose tissue between the MICT and SED groups

	MICT/SED						
	RT	VIP[a]	FC[b]	Log (FC)[c]	*p* value[d]	MF	Category
Glycerol	9.17	2.615	1.767	0.25	0.025	90.59	Lipid metabolism
1-Heptadecanol	18.24	4.1	0.748	− 0.13	0.011	81.48	Lipid metabolism
Palmitic acid	18.23	5.366	0.578	− 0.24	0.0001	84.66	Lipid metabolism
Palmitoleic acid	18.03	1.175	0.443	− 0.35	0.0005	83.26	Lipid metabolism
Stearic acid	20.04	2.513	0.458	− 0.34	5.95E−05	86.58	Lipid metabolism
Octadecadienoic acid	19.76	2.309	0.298	− 0.53	4.96E−05	91.88	Lipid metabolism
Urea	8.76	1.016	0.346	− 0.46	0.011	83.54	Amino acid metabolism
Lumichrome	10.02	1.368	1.31	0.12	0.02	94.34	Oxidative stress
Alpha-tocopherol	27.12	2.747	2.044	0.31	0.047	97.54	Oxidative stress

SED sedentary control, *MICT* moderate-intensity continuous training, *RT* retention time, *VIP* variable importance in the projection, *FC* fold change, *MF* match factor

[a] Only metabolites with VIP values of greater than 1.0

[b] Fold change was calculated as the logarithm of the average mass response (area)

[c] Ratio between the two classes (i.e., fold change = $\log_2$[MICT/SED]); positive and negative values indicate higher and lower levels in MICT

[d] $P < 0.05$ was considered statistically significant by Student's *t* test

induced by MICT, whereas cholesterol was specifically upregulated by HIIT, suggesting that HIIT and MICT interventions had different effects on metabolic changes in adipose tissue in aged rats.

Palmitic acid, octadecadienoic acid, and stearic acid are three major free fatty acids in adipose tissue. Palmitic acid is the most abundant circulating saturated fatty acid and the main product of de novo lipogenesis in positive energy balance; thus, increasing dietary palmitic acid causes decreased fat oxidation and increased body fat gain during lipogenesis [20]. In a sedentary lifestyle, palmitic acid has detrimental health effects, and accumulation of tissue palmitic acid results in dyslipidemia, hyperglycemia, and increased ectopic fat accumulation, further accelerating these deleterious effects [8]. Moreover, **8** weeks of endurance exercise reduces palmitic acid content in white adipose tissue in male SD rats at 6 weeks of age [31]. A previous study showed that decreased palmitic acid contents are associated with the alleviation of obesity-related features [10], such as reduced visceral adiposity. Stearic acid, an intermediate in mitochondrial β-oxidation of long-chain saturated fatty acids, is involved in the regulation of adipogenesis and lipogenesis and tends to be associated with decreased cardiovascular disease risk [18]. We also observed decreased body fat gain following HIIT and a

Table 4 Changes of the metabolites in adipose tissue between HIIT and SED groups

Metabolites	HIIT/SED						
	RT	VIP[a]	FC[b]	Log(FC)[c]	*P* value[d]	MF	Category
Cholesterol	27.24	4.124	3.506	0.545	0.006	84.82	Lipid metabolism
Palmitic acid	18.23	4.038	0.784	− 0.106	0.012	84.66	Lipid metabolism
Stearic acid	20.04	2.224	0.644	− 0.191	0.004	86.58	Lipid metabolism
Octadecadienoic acid	19.76	2.171	0.499	− 0.302	0.002	91.88	Lipid metabolism
Lumichrome	10.02	2.089	1.458	0.164	0.01	94.34	Oxidative stress
Alpha-tocopherol	27.12	3.73	2.285	0.359	0.04	97.54	Oxidative stress

SED sedentary control, *HIIT* high-intensity interval training, *RT* retention time, *VIP* variable importance in the projection, *FC* fold change, *MF* match factor

[a] Only metabolites with VIP values of greater than 1.0

[b] Fold change was calculated as the logarithm of the average mass response (area)

[c] Ratio between the two classes (i.e., fold change = $\log_2$[HIIT/SED]); positive and negative values indicate higher and lower levels in HIIT

[d] $P < 0.05$ was considered statistically significant by Student's *t* tests

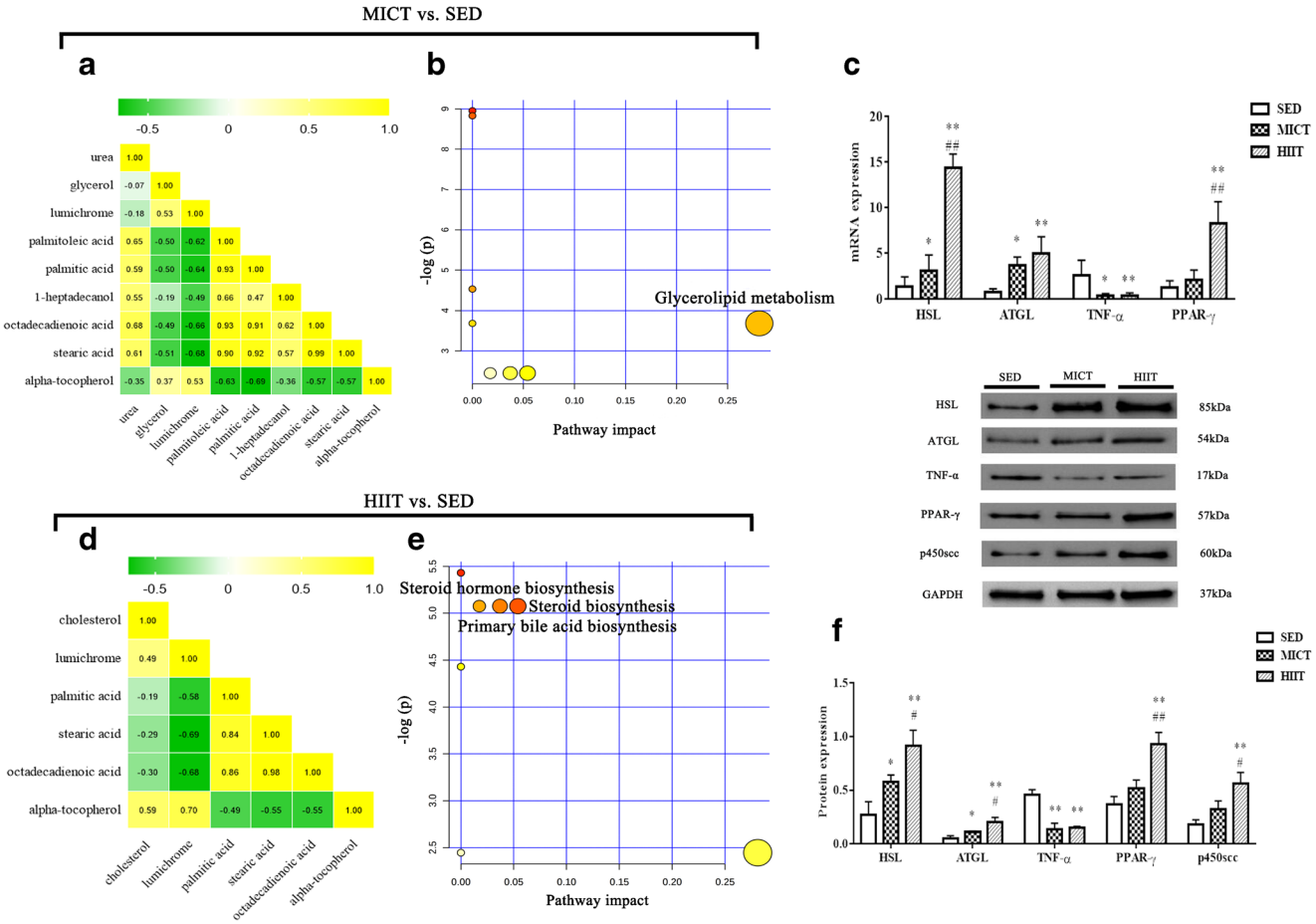

Fig. 4 Metabolic pathway enrichment analysis and lipolysis metabolism-related protein and mRNA expression. Correlation analysis of 9 metabolites (**a**); metabolic pathway analysis in MICT versus SED (**b**); mRNA levels of PPAR-γ, HSL, ATGL, and TNF-α in adipose tissues (**c**); correlation analysis of 6 metabolites (**d**); metabolic pathway analysis in HIIT versus SED (**e**); and contents of PPAR-γ, HSL, ATGL, TNF-α, and P450scc protein (**f**). SED sedentary control group, MICT moderate-intensity continuous training group, HIIT high-intensity interval training group, PPAR-γ peroxisome proliferator activated receptor gamma, HSL hormone-sensitive lipase, ATGL adipose triacylglyceride lipase, TNF-α tumor necrosis factor-alpha, P450scc cholesterol-side-chain cleavage enzyme. The data were analyzed by one-way ANOVA followed by Tukey's post-hoc test. Data are presented as means ± SD. $^{*}P < 0.05$ versus SED; $^{**}P < 0.01$ versus SED; $^{\#}P < 0.05$ versus MICT; $^{\#\#}P < 0.01$ versus MICT

decreased tendency for body fat gain following MICT, which may be associated with reduced production of palmitic acid and stearic acid, from aging PAT (Table 5). Additionally, stearic acid enhances lipogenesis during the maturation stages of bovine adipocyte and blocks lipolysis by decreasing key lipolytic enzyme *ATGL* mRNA [39]. Indeed, age-related defective lipolysis is associated with inhibition of key lipolytic enzymes, such as adipose ATGL and HSL, resulting in defective FFA mobilization and reduced levels of circulating FFA in the elderly [6].

Our current study showed that both exercise modalities induced ATGL and HSL mRNA and protein expression in the PAT, whereas circulating FFA and adipocyte sizes were significantly increased and reduced, respectively, in the HIIT group when compared with the SED group, consistent with a study in aged hamsters by Campbell et al. [7], who showed that exercise-induced weight loss and lipolysis increase the expression of HSL and ATGL protein in perirenal and subcutaneous adipose tissue. Furthermore, PPAR-γ may also coordinate the balance between fat deposition and mobilization through its effects on upregulation of ATGL and HSL expression in adipose tissue [24, 32, 33]. In the current study, HIIT increased *PPAR-γ* mRNA and protein expression in the PAT, and upregulation of *PPAR-γ* mRNA was positively correlated with *HSL* mRNA, *ATGL* mRNA, and circulating FFA (Table 5). These findings were consistent with a previous study demonstrating that PPAR-γ activation upregulated *ATGL* and *HSL* mRNA in 3T3-L1 adipocytes [32], supporting the hypothesis that PPAR-γ may be required for HIIT to promote ATGL and HSL expression in aging adipose tissue.

In this study, α-tocopherol, a lipid-soluble antioxidant that protects cell membranes from oxidative attack, was significantly increased in both exercise modalities. Our previous study demonstrated that 4-hydroxynonenal and 8-

Table 5 Correlation analysis among various parameters

	Maximum run speed	Exhaustion to time	FFA	PPAR-gamma mRNA	HSL mRNA	ATGL mRNA	Stearic acid	Alpha-tocopherol
Maximum run speed		0.98**	0.45	0.10	0.18	0.29	− 0.76**	0.48*
Exhaustion to time	0.98**		0.50*	0.19	0.29	0.46	− 0.78 **	0.46*
FFA	0.45	0.50*		0.89**	0.86**	0.63 *	− 0.48 *	0.43
PPAR-gamma mRNA	0.10	0.19	0.89**		0.93**	0.74 **	− 0.24	0.03
HSL mRNA	0.18	0.29	0.86**	0.93**		0.76 *	− 0.27	− 0.05
ATGL mRNA	0.29	0.46	0.63*	0.74**	0.76*		− 0.59*	0.27
Stearic acid	− 0.76**	− 0.78**	− 0.48*	− 0.24	− 0.27	− 0.59*		− 0.50*
alpha-Tocopherol	0.48*	0.46*	0.43	0.03	− 0.05	0.27	− 0.50*	

*$P < 0.05$; **$P < 0.01$

hydroxydeoxyguanosine decreased significantly after MICT and HIIT in serum and skeletal muscle [22]. Indeed, oxidative stress biomarkers, such as H_2O_2, were reduced in tocopherol-treated animals, whereas antioxidants, such as superoxide dismutase 2, were upregulated [4]. Our current findings were consistent with those of a previous study showing increases in plantaris α-tocopherol analyzed by GC/MS following endurance exercise [37]. In cross-sectional studies, higher plasma α-tocopherol levels were found to be associated with greater grip and knee strength in elderly women [35]. Previous studies have shown that α-tocopherol improves mitochondrial efficiency, muscle mass, muscle contractile properties, and exercise capacity, thus attenuating sarcopenia in humans [9]. Furthermore, our current data demonstrated that elevation of α-tocopherol in aging adipose tissue was positively correlated with exhaustion to time and maximum run speed (Table 5). Thus, both exercise modalities improved muscle function or mitigated functional decline during aging, and these effects could be mediated by α-tocopherol-dependent suppression of age-related oxidative stress. Lumichrome, a photodegradation product of riboflavin, is important in cellular oxidation and energy metabolism. Lumichrome and riboflavin have protective effects against ischemia-reperfusion injury in rat hearts, and supplementation with dietary riboflavin results in significant amelioration of oxidative stress in white adipose tissue [2]. Thus, the roles of lumichrome in alleviation of oxidative stress in aging adipose tissue, particularly during exercise training, should be evaluated in future studies.

Palmitoleic acid, urea, 1-heptadecanol, and glycerol were specifically altered by MICT. Palmitoleic acid, an unsaturated fatty acid, is formed from palmitic acid by desaturation via stearoyl-CoA desaturase 1 activity and is associated with increased risk of myocardial infarction [18]. Our current findings were consistent with a previous report demonstrating that endurance-training interventions decreased palmitoleic acid in visceral adipose tissue in the high fat diet-fed groups and standard rats [31]. Glycerol, an intermediate of glycerolipid metabolism, has important primary functions in adipocytes involving mobilized triglycerides when energy demands arise [7]. In this study, we observed increased levels of glycerol in visceral adipose tissue, consistent with our biochemical analysis of plasma FFA levels in the MICT and SED groups, supporting the metabolism of triglycerides through the hydrophilic metabolite glycerol from adipose tissue. As previously described, endurance training decreases adipose tissue mass and increases lipolytic rates in older hamsters [7]. These results supported our finding that MICT may upregulate lipolysis through a postreceptor mechanism, possibly involving HSL and ATGL, in aged adipose tissue. Additionally, we could not differentiate 1-heptadecanol, a long-chain alcohol, from exogenously provided heptadecanoic acid, which is a fatty acid of exogenous origin found in adipose tissue [18]. Although the potential role of 1-heptadecanol is unclear, heptadecanoic acid is inversely associated with mortality [18]. In addition, white adipose tissue can convert 2-amino N to ammonium and finally urea, particularly under conditions of obesity/inflammation [28], indeed, an increase in white adipose tissue mass and upregulation of genes related to the urea cycle [1, 28]. These results supported our finding that MICT may downregulate urea levels and the urea cycle in PAT possibly involving a decrease in adipose tissue mass.

Upregulation of cholesterol was specifically induced by HIIT. Although cholesterol is a known risk factor of arteriosclerosis, particularly in the context of obesity, this metabolite is a valuable source of metabolic energy and participates in membrane synthesis and steroid hormone biosynthesis, thereby contributing to anti-inflammatory effects and glycolipid metabolism [7]. As is shown in Fig. 5, the conversion of cholesterol to pregnenolone by p450scc, a rate-limiting step of steroid hormone biosynthesis, results in progressive decline in aged mice and subsequent decrease in steroidogenesis [16]. One anti-inflammatory mechanism of action for exercise training may be its stimulation of endogenous corticosterone secretion in obese mice [12] and old Syrian golden hamsters [7, 11] via its function as a natural anti-inflammatory agent

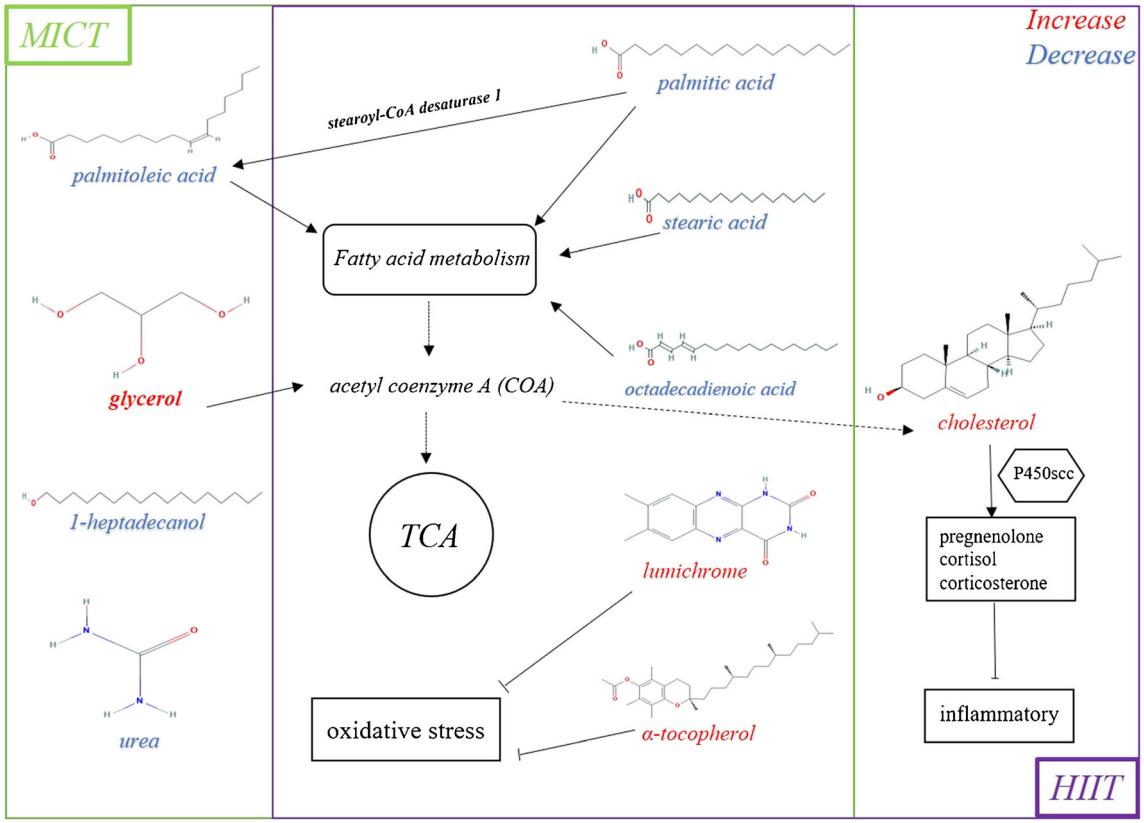

Fig. 5 Summary of metabolic alterations in adipose tissue of aging rats upon HIIT and MICT. Note: Red and blue fonts indicate increases and decreases in the levels of the metabolites in aging rats, respectively

against various types of stress. Surprisingly, in our study, these metabolites were mainly involved in steroid hormone biosynthesis in the HIIT group, and p450scc protein levels were increased in the PAT. Moreover, serum and PAT pregnenolone, cortisol, and corticosterone were elevated accompanied with lower serum hsCRP levels and adipose tissue pro-inflammatory factor TNF-α expression, and higher serum anti-inflammatory factor IL-10 levels in the HIIT group compared with those in the SED group, suggesting that HIIT may favorably regulate anti-inflammatory activity via steroid hormone biosynthesis pathways. Furthermore, in our study, we observed downregulation of leptin, a pro-inflammatory factor, and increases in estradiol levels, but not adiponectin levels, in PAT. Both of these molecules are anti-inflammatory factors found in PAT after HIIT and have anti-inflammatory effects associated with increased IL-10 production in the serum [23]. Taken together, the results of the current study strongly support a HIIT-induced moderate increase in corticosterone concentrations by P450scc-meditated steroid hormone biosynthesis, which may protect against age-related inflammation.

Both exercise modalities shared common metabolic pathways involved in glycerolipid metabolism, whereas MICT did not have strong anti-inflammatory effects. The results were consistent with a study of high-fat diet-induced obese animals, indicating that adipose tissue glycolipid metabolism, but not the anti-inflammatory phenotype, was altered in response to endurance training [31]. Owing to the complexity of the data, we cannot explain why both exercise modalities shared common metabolic pathways with the SED group. However, this was the first substantial study of exercise-induced metabolomics in aged adipose tissue, and further studies are needed to elucidate the involvement of metabolic pathways associated with inflammation and lipid metabolism in aged adipose tissues following HIIT or MICT.

Because this was a descriptive study, there were some limitations that should be discussed. First, preclinical and human studies are needed to fully characterize the different benefits of HIIT compared with those of volume-matched MICT. Second, metabolomic profiling and physiological adaptations of adipose tissue types, such as subcutaneous fat, should be performed under different exercise training protocols. Additionally, our study was restricted to female rats, and we cannot exclude the possibility that PAT metabolomic profiles may differ in male rats. Indeed, sex steroid hormone production by adipose tissues differs between sexes during aging, and age-associated declines in estrogen are more prominent in females [5]. Based on translational significance and practical implications, we used female rats that were naturally aged (18 months of age) because these rats have been shown to better reflect changes in estrogen metabolism during exercise

training that may protect against age-related inflammation and metabolic disorders. Finally, the exact mechanisms were not directly determined; therefore, future studies are required to identify associations between inflammation and PAT metabolites involved in lipolysis induced by HIIT and MICT.

Conclusions

In summary, our findings provided insights into the distinct differences in specific metabolites, body composition, adipocytokines, lipolysis metabolism, and inflammation-related markers induced by HIIT versus MICT and highlighted the value of metabolomic analysis for elucidating the contributions of HIIT to regulation of anti-inflammatory activity via steroid hormone biosynthesis pathways in aging adipose tissue.

Author contributions L.F.H., S.L., and L.T. designed the study. L.F.H., S.L., L.T., M.Z., Y.L.D., G.H.E., W.D.S., and X.T. collected the data and carried out data analyses. L.F.H. and S.L. prepared the figures and produced the initial draft of the manuscript. All authors read and approved the final submitted manuscript.

Funding information This study was supported by the National Natural Science Foundation of China (grant no. 31500961 and 31971099), Guangdong Scientific Project (grant nos. 2014A020220015 and 2015A020219015), the Natural Science Fund for Colleges and Universities of Jiangsu Province (grant no. 18KJB180011), Priority Academic Program Development of Jiangsu Higher Education Institutions (PAPD), and the Postgraduate Research & Practice Innovation Program of Jiangsu Province (grant no. KYCX19_0774).

Compliance with ethical standards All experiments were approved by the Ethics Committee on Animal Experimentation of the Guangdong Medical Laboratory Animal Center and followed the Guidelines for the Care and Use of Laboratory Animals. Experiments were approved by the Animal Experiment Ethical Inspection Form of Nanjing Normal University (IACUU-1903006).

Conflict of interest The authors declare that they have no conflict of interest.

References

1. Adam J, Brandmaier S, Leonhardt J, Scheerer MF, Mohney RP, Xu T, Bi J, Rotter M, Troll M, Chi S, Heier M, Herder C, Rathmann W, Giani G, Adamski J, Illig T, Strauch K, Li Y, Gieger C, Peters A, Suhre K, Ankerst D, Meitinger T, Hrabe de Angelis M, Roden M, Neschen S, Kastenmuller G, Wang-Sattler R (2016) Metformin effect on nontargeted metabolite profiles in patients with type 2 diabetes and in multiple murine tissues. Diabetes 65:3776–3785. https://doi.org/10.2337/db16-0512
2. Alam MM, Iqbal S, Naseem I (2015) Ameliorative effect of riboflavin on hyperglycemia, oxidative stress and DNA damage in type-2 diabetic mice: mechanistic and therapeutic strategies. Arch Biochem Biophys 584:10–19. https://doi.org/10.1016/j.abb.2015.08.013
3. Aldiss P, Symonds ME, Lewis JE, Boocock DJ, Miles AK, Bloor I, Ebling FJP, Budge H (2019) Interscapular and perivascular Brown adipose tissue respond differently to a short-term high-fat diet. Nutrients 11. https://doi.org/10.3390/nu11051065
4. Aragno M, Mastrocola R, Catalano MG, Brignardello E, Danni O, Boccuzzi G (2004) Oxidative stress impairs skeletal muscle repair in diabetic rats. Diabetes 53:1082–1088. https://doi.org/10.2337/diabetes.53.4.1082
5. Burger HG, Hale GE, Dennerstein L, Robertson DM (2008) Cycle and hormone changes during perimenopause: the key role of ovarian function. Menopause 15:603–612. https://doi.org/10.1097/gme.0b013e318174ea4d
6. Camell CD, Sander J, Spadaro O, Lee A, Nguyen KY, Wing A, Goldberg EL, Youm YH, Brown CW, Elsworth J, Rodeheffer MS, Schultze JL, Dixit VD (2017) Inflammasome-driven catecholamine catabolism in macrophages blunts lipolysis during ageing. Nature 550:119–123. https://doi.org/10.1038/nature24022
7. Campbell JE, Fediuc S, Hawke TJ, Riddell MC (2009) Endurance exercise training increases adipose tissue glucocorticoid exposure: adaptations that facilitate lipolysis. Metab Clin Exp 58:651–660. https://doi.org/10.1016/j.metabol.2009.01.002
8. Carta G, Murru E, Banni S, Manca C (2017) Palmitic acid: physiological role, metabolism and nutritional implications. Front Physiol 8:902. https://doi.org/10.3389/fphys.2017.00902
9. Chung E, Mo H, Wang S, Zu Y, Elfakhani M, Rios SR, Chyu MC, Yang RS, Shen CL (2018) Potential roles of vitamin E in age-related changes in skeletal muscle health. Nutr Res 49:23–36. https://doi.org/10.1016/j.nutres.2017.09.005
10. Coelho DF, Pereira-Lancha LO, Chaves DS, Diwan D, Ferraz R, Campos-Ferraz PL, Poortmans JR, Lancha Junior AH (2011) Effect of high-fat diets on body composition, lipid metabolism and insulin sensitivity, and the role of exercise on these parameters. Braz J Med Biol Res 44:966–972. https://doi.org/10.1590/s0100-879x2011007500107
11. Coutinho AE, Fediuc S, Campbell JE, Riddell MC (2006) Metabolic effects of voluntary wheel running in young and old Syrian golden hamsters. Physiol Behav 87:360–367. https://doi.org/10.1016/j.physbeh.2005.10.006
12. Du SF, Yu Q, Chuan K, Ye CL, He ZJ, Liu SJ, Zhu XY, Liu YJ (2017) In obese mice, exercise training increases 11beta-HSD1 expression, contributing to glucocorticoid activation and suppression of pulmonary inflammation. J Appl Physiol 123:717–727. https://doi.org/10.1152/japplphysiol.00652.2016
13. Elhakeem A, Hannam K, Deere KC, Hartley A, Clark EM, Moss C, Edwards MH, Dennison E, Gaysin T, Kuh D, Wong A, Cooper C, Cooper R, Tobias JH (2018) Physical activity producing low, but not medium or higher, vertical impacts is inversely related to BMI in older adults: findings from a multicohort study. J Gerontol A Biol Sci Med Sci 73:643–651. https://doi.org/10.1093/gerona/glx176
14. Fazelzadeh P, Hangelbroek RW, Tieland M, de Groot LC, Verdijk LB, van Loon LJ, Smilde AK, Alves RD, Vervoort J, Muller M, van Duynhoven JP, Boekschoten MV (2016) The muscle metabolome differs between healthy and frail older adults. J Proteome Res 15:499–509. https://doi.org/10.1021/acs.jproteome.5b00840
15. Giesbertz P, Padberg I, Rein D, Ecker J, Hofle AS, Spanier B, Daniel H (2015) Metabolite profiling in plasma and tissues of ob/ob and db/db mice identifies novel markers of obesity and type 2 diabetes. Diabetologia 58:2133–2143. https://doi.org/10.1007/s00125-015-3656-y
16. Huang D, Wei W, Xie F, Zhu X, Zheng L, Lv Z (2018) Steroidogenesis decline accompanied with reduced antioxidation and endoplasmic reticulum stress in mice testes during ageing. Andrologia:50. https://doi.org/10.1111/and.12816
17. Huffman DM, Barzilai N (2009) Role of visceral adipose tissue in aging. Biochim Biophys Acta 1790:1117–1123. https://doi.org/10.1016/j.bbagen.2009.01.008

18. Iggman D, Arnlov J, Cederholm T, Riserus U (2016) Association of adipose tissue fatty acids with cardiovascular and all-cause mortality in elderly men. JAMA Cardiol 1:745–753. https://doi.org/10.1001/jamacardio.2016.2259
19. Kiehn JT, Tsang AH, Heyde I, Leinweber B, Kolbe I, Leliavski A, Oster H (2017) Circadian rhythms in adipose tissue physiology. Comprehens Physiol 7:383–427. https://doi.org/10.1002/cphy.c160017
20. Kien CL, Bunn JY, Ugrasbul F (2005) Increasing dietary palmitic acid decreases fat oxidation and daily energy expenditure. Am J Clin Nutr 82:320–326. https://doi.org/10.1093/ajcn.82.2.320
21. Larsen S, Danielsen JH, Sondergard SD, Sogaard D, Vigelsoe A, Dybboe R, Skaaby S, Dela F, Helge JW (2015) The effect of high-intensity training on mitochondrial fat oxidation in skeletal muscle and subcutaneous adipose tissue. Scand J Med Sci Sports 25:e59–e69. https://doi.org/10.1111/sms.12252
22. Li FH, Sun L, Zhu M, Li T, Gao HE, Wu DS, Zhu L, Duan R, Liu TC (2018) Beneficial alterations in body composition, physical performance, oxidative stress, inflammatory markers, and adipocytokines induced by long-term high-intensity interval training in an aged rat model. Exp Gerontol 113:150–162. https://doi.org/10.1016/j.exger.2018.10.006
23. Mela V, Hernandez O, Hunsche C, Diaz F, Chowen JA, De la Fuente M (2017) Administration of a leptin antagonist during the neonatal leptin surge induces alterations in the redox and inflammatory state in peripubertal/adolescent rats. Mol Cell Endocrinol 454:125–134. https://doi.org/10.1016/j.mce.2017.06.018
24. Mennes E, Dungan CM, Frendo-Cumbo S, Williamson DL, Wright DC (2014) Aging-associated reductions in lipolytic and mitochondrial proteins in mouse adipose tissue are not rescued by metformin treatment. J Gerontol A Biol Sci Med Sci 69:1060–1068. https://doi.org/10.1093/gerona/glt156
25. Norheim F, Langleite TM, Hjorth M, Holen T, Kielland A, Stadheim HK, Gulseth HL, Birkeland KI, Jensen J, Drevon CA (2014) The effects of acute and chronic exercise on PGC-1alpha, irisin and browning of subcutaneous adipose tissue in humans. FEBS J 281:739–749. https://doi.org/10.1111/febs.12619
26. Nunes PRP, Martins FM, Souza AP, Carneiro MAS, Orsatti CL, Michelin MA, Murta EFC, de Oliveira EP, Orsatti FL (2019) Effect of high-intensity interval training on body composition and inflammatory markers in obese postmenopausal women: a randomized controlled trial. Menopause 26:256–264. https://doi.org/10.1097/gme.0000000000001207
27. Palmer AK, Kirkland JL (2016) Aging and adipose tissue: potential interventions for diabetes and regenerative medicine. Exp Gerontol 86:97–105. https://doi.org/10.1016/j.exger.2016.02.013
28. Plubell DL, Wilmarth PA, Zhao Y, Fenton AM, Minnier J, Reddy AP, Klimek J, Yang X, David LL, Pamir N (2017) Extended multiplexing of tandem mass tags (TMT) labeling reveals age and high fat diet specific proteome changes in mouse epididymal adipose tissue. Molec Cell Proteomics 16:873–890. https://doi.org/10.1074/mcp.M116.065524
29. Redman LM, Smith SR, Burton JH, Martin CK, Il'yasova D, Ravussin E (2018) Metabolic slowing and reduced oxidative damage with sustained caloric restriction support the rate of living and oxidative damage theories of aging. Cell Metab 27(805–815):e804. https://doi.org/10.1016/j.cmet.2018.02.019
30. Robinson MM, Dasari S, Konopka AR, Johnson ML, Manjunatha S, Esponda RR, Carter RE, Lanza IR, Nair KS (2017) Enhanced protein translation underlies improved metabolic and physical adaptations to different exercise training modes in young and old humans. Cell Metab 25:581–592. https://doi.org/10.1016/j.cmet.2017.02.009
31. Rocha-Rodrigues S, Rodriguez A, Goncalves IO, Moreira A, Maciel E, Santos S, Domingues MR, Fruhbeck G, Ascensao A, Magalhaes J (2017) Impact of physical exercise on visceral adipose tissue fatty acid profile and inflammation in response to a high-fat diet regimen. Int J Biochem Cell Biol 87:114–124. https://doi.org/10.1016/j.bioce1.2017.04.008
32. Rodriguez-Cuenca S, Carobbio S, Velagapudi VR, Barbarroja N, Moreno-Navarrete JM, Tinahones FJ, Fernandez-Real JM, Oresic M, Vidal-Puig A (2012) Peroxisome proliferator-activated receptor gamma-dependent regulation of lipolytic nodes and metabolic flexibility. Mol Cell Biol 32:1555–1565. https://doi.org/10.1128/mcb.06154-11
33. Savage DB, Tan GD, Acerini CL, Jebb SA, Agostini M, Gurnell M, Williams RL, Umpleby AM, Thomas EL, Bell JD, Dixon AK, Dunne F, Boiani R, Cinti S, Vidal-Puig A, Karpe F, Chatterjee VK, O'Rahilly S (2003) Human metabolic syndrome resulting from dominant-negative mutations in the nuclear receptor peroxisome proliferator-activated receptor-gamma. Diabetes 52:910–917. https://doi.org/10.2337/diabetes.52.4.910
34. Schafer MJ, White TA, Evans G, Tonne JM, Verzosa GC, Stout MB, Mazula DL, Palmer AK, Baker DJ, Jensen MD, Torbenson MS, Miller JD, Ikeda Y, Tchkonia T, van Deursen JM, Kirkland JL, LeBrasseur NK (2016) Exercise prevents diet-induced cellular senescence in adipose tissue. Diabetes 65:1606–1615. https://doi.org/10.2337/db15-0291
35. Semba RD, Blaum C, Guralnik JM, Moncrief DT, Ricks MO, Fried LP (2003) Carotenoid and vitamin E status are associated with indicators of sarcopenia among older women living in the community. Aging Clin Exp Res 15:482–487
36. Sogaard D, Lund MT, Scheuer CM, Dehlbaek MS, Dideriksen SG, Abildskov CV, Christensen KK, Dohlmann TL, Larsen S, Vigelso AH, Dela F, Helge JW (2018) High-intensity interval training improves insulin sensitivity in older individuals. Acta Physiol 222:e13009. https://doi.org/10.1111/apha.13009
37. Starnes JW, Parry TL, O'Neal SK, Bain JR, Muehlbauer MJ, Honcoop A, Ilaiwy A, Christopher PM, Patterson C, Willis MS (2017) Exercise-induced alterations in skeletal muscle, heart, liver, and serum metabolome identified by non-targeted metabolomics analysis. Metabolites 7. https://doi.org/10.3390/metabo7030040
38. Wang N, Liu Y, Ma Y, Wen D (2017) High-intensity interval versus moderate-intensity continuous training: superior metabolic benefits in diet-induced obesity mice. Life Sci 191:122–131. https://doi.org/10.1016/j.lfs.2017.08.023
39. Yanting C, Yang QY, Ma GL, Du M, Harrison JH, Block E (2018) Dose- and type-dependent effects of long-chain fatty acids on adipogenesis and lipogenesis of bovine adipocytes. J Dairy Sci 101:1601–1615. https://doi.org/10.3168/jds.2017-13312